Complete Bond Force Fields for Trivalent and Deltahedral Cages: Group Theory and Applications to Cubane, Closo-dodecaborane, and Buckminsterfullerene

Arnout Ceulemans,* Bruno C. Titeca,† Liviu F. Chibotaru, and Ingrid Vos

Division of Quantum Chemistry, Katholieke Universiteit Leuven, Celestijnenlaan 200F, B-3001 Heverlee (Leuven), Belgium

Patrick W. Fowler

School of Chemistry, University of Exeter, Stocker Rd., Exeter EX4 4QD, UK

Received: October 6, 2000; In Final Form: June 27, 2001

Group theory is used to define complete force fields for deltahedral and trivalent molecular skeletons in terms of bond stretches, and bond stretches and slides, respectively. Analysis of ab initio Hessian matrices shows the delocalized nature of the force field in boranes and the relatively localized force field in C_{60}, where only interactions of bonds in adjacent rings or separated by at most three edges of the truncated icosahedron show significant interaction.

1. Introduction

Is the force field in carbon and boron clusters local, or does it have long-range components? What is the best choice of internal coordinates for three-dimensional cage molecules? How should one analyse and compare first-principles calculations of the Hessian matrix for clusters?

The core of these questions is the problem of coordinates. One needs to find a set of suitable coordinates, which is based on the topology of the cluster. In the present paper, we show how such coordinates can be defined for deltahedral clusters and their trivalent duals. The treatment makes use of two group-theoretical theorems which relate the mechanical representation of such clusters to their topology.[1] In this coordinate basis, we construct a complete force field, which fully characterizes the chemical bonding. A complete force field precisely covers the information which is contained in frequencies and composition of the normal modes. It thus represents the exact inverse of the vibrational eigenvalue problem. The theoretical results are applied to explicit calculations on highly symmetrical representative cages of carbon and boron.

2. Group-Theoretical and Topological Background

Consider a polyhedral cluster with v vertex points or atoms. The set of all vertexes spans a reducible representation of the molecular point group. We shall refer to this as the positional representation, $\Gamma_\sigma(v)$. The σ index is a cylindrical label, which indicates that the vertex points are invariant with respect to all symmetry elements that pass through the atom sites. Tables of $\Gamma_\sigma(v)$ for many symmetric clusters are available in the literature.[2]

From its equilibrium position, each atom can move in three orthogonal Cartesian directions. The set of $3v$ displacements spans the mechanical representation of the cluster, $\Gamma_M(v)$. According to induction theory,[3] the mechanical representation is obtained by forming the direct product of the positional representation with that of the three translations

$$\Gamma_M(v) = \Gamma_\sigma(v) \times \Gamma_T \tag{1}$$

It includes the six collective modes, three translations, and three rotations, transforming, respectively, as Γ_T and Γ_R. Subtracting these, we obtain the symmetry representation of the internal modes of vibration, $\Gamma_{vib}(v)$:

$$\Gamma_{vib}(v) = \Gamma_M(v) - \Gamma_T - \Gamma_R, \tag{2}$$

which covers the $3v - 6$ internal degrees of freedom of a nonlinear molecule with v atoms. Using standard group-theoretical techniques, $\Gamma_{vib}(v)$ may be resolved into irreducible representations, describing the internal symmetry coordinates.[4] In principle, several types of symmetry coordinates exist, e.g., bond stretches, changes in bond angles, dihedral angles, etc., and the problem is to find a suitable minimal set that reflects the bonding most efficiently.

A special symmetry relationship can be obtained for a specific class of clusters: the deltahedra. All faces of a deltahedron are triangles. This is the favored bonding mode adopted by boron in the closo-borane, $B_nH_n^{2-}$, series.[5] For deltahedra, the number of vertexes, v, is related to the number of edges or bonds, e, by

$$3v - 6 = e. \tag{3}$$

This counting rule has a symmetry extension, which forms the key group-theoretical theorem for the construction of force fields in boron cages. The extension is obtained by replacing each term in the counting rule by an appropriate symmetry representation, yielding[1]

$$\Gamma_T \times \Gamma_\sigma(v) - \Gamma_T - \Gamma_R = \Gamma_\sigma(e). \tag{4}$$

or, on substitution

$$\Gamma_{vib}(v) = \Gamma_\sigma(e). \tag{5}$$

The term $\Gamma_\sigma(e)$ in this result is the symmetry representation

* Corresponding author. Tel.: +32-16-32.73.63. Fax: +32-16-32.79.92. E-mail: Arnout.Ceulemans@chem.kuleuven.ac.be.

† Current address: BarcoView nv, Kortrijk, Belgium.

10.1021/jp0036792 CCC: $20.00
Published on Web 08/17/2001

spanned by all stretches of the edge bonds. Such stretches are, indeed, fully symmetric or σ-type objects with respect to the symmetry elements passing through the edge midpoints. Hence, the result in eq 5 states that the internal modes of vibration and the stretches of the bonds of a deltahedron span the same symmetry. We can thus construct a complete harmonic force field for deltahedral clusters taking all possible interactions between edge bonds. As compared to the conventional Cartesian Hessian, which is of course also complete, a bond force field has the advantage that it is based on symmetry-equivalent interactions and thus corresponds to the simplest symmetry representation of elastic forces in a molecule. In addition, it gives direct information on the chemical bonding.

This relationship was found by Boyle and Parker[6] in a study of closo-$B_{12}H_{12}^{2-}$ but taken as a coincidence of icosahedral symmetry. It was shown later to be true for all deltahedra that can be mapped on the surface of a sphere.[1] In mechanical terms, the theorem implies that a deltahedron cannot vibrate unless some of its bond lengths are changing. In this form, it is a consequence of a general result, which was obtained by the famous French polymath Cauchy[7] as early as 1812, and states that "Every convex polyhedral surface with rigid faces is inflexible". [II^e Mémoire sur les Polygones et les Polyèdres, Théorème XIII: "*Dans un polyèdre convexe, dont toutes les faces sont invariables, les coins compris entre les faces, ou, ce qui revient au même, les inclinaisons sur les différentes arêtes sont aussi invariables*". ("In a convex polyhedron with rigid faces, the angles between the faces—or, in other words, the inclinations on the different edges—will also be rigid".) Since the proof of the completeness of the set of stretching coordinates as internal modes rests on Euler's theorem, it is really a topological property of deltahedra. This implies that even in the absence of all symmetry the bond stretches of a convex deltahedron form a complete nonredundant set of internal coordinates. In the next section, we will use this result to construct a complete force field for deltahedral clusters.

The dual of a deltahedron is a trivalent cluster in which three bonds radiate from each atom. This is the preferred bonding mode of carbon, both in the polyhedranes, C_nH_n, and in the fullerenes, C_n. For trivalent clusters, the counting rule is

$$3v = 2e \tag{6}$$

Again, there is a symmetry extension in which each term is replaced by its symmetry representation. This forms our second group-theoretical relation:[1]

$$\Gamma_T \times \Gamma_\sigma(v) = \Gamma_\sigma(e) + \Gamma_{||}(e) \tag{7}$$

or, on substitution

$$\Gamma_M(v) = \Gamma_\sigma(e) + \Gamma_{||}(e). \tag{8}$$

Here, $\Gamma_{||}(e)$ is the symmetry representation of a set of vectors or arrows, one along each bond. The right-hand side of the equation thus represents the symmetry of all edge stretches and edge-sliding movements (or "slides", for short). This is found to match the mechanical representation, but now, in contrast with the case of deltahedral clusters, the symmetries of the six collective modes are included in the edge slides, $\Gamma_{||}(e)$. On the basis of this theorem, we can thus construct a complete force field for trivalent clusters in terms of bond stretches and slides but must take into account some redundancy relations for the slide constants. This construction will be presented in section 4.

3. Complete Force Field for Deltahedra

We now proceed to the construction of a complete force field for deltahedra and the identification of the force constants. We will assume that the cluster consists of v identical atoms or superatoms with mass m. Let (x_i^e, y_i^e, z_i^e) denote the equilibrium position of atom i ($i = 1, ..., v$). The displacements of each atom with respect to its equilibrium position in the three Cartesian directions of a common coordinate frame will be denoted by nonsuperscripted symbols x_i, y_i, and z_i. These form the basis set of the mechanical representation. For general purposes, an element of this set will be referred to as q_k, with $k = 1, ..., 3v$. In addition, we define a set of internal coordinates s_I: the first $3v - 6$ elements of this set correspond to all bond stretches, $\Delta r_{\langle ij \rangle}$, of the deltahedron, and the remaining six elements are the translations and rotations. It is convenient to group both types of coordinates in column vectors as

$$\mathbf{q} = \begin{pmatrix} x_1 \\ y_1 \\ z_1 \\ x_2 \\ y_2 \\ z_2 \\ \vdots \\ x_v \\ y_v \\ z_v \end{pmatrix}, \qquad \mathbf{s} = \begin{pmatrix} \Delta r_{\langle 12 \rangle} \\ \Delta r_{\langle 13 \rangle} \\ \vdots \\ T_x \\ T_y \\ T_z \\ R_x \\ R_y \\ R_z \end{pmatrix} \tag{9}$$

The bond between atoms i and j is denoted as $\langle ij \rangle$. The stretching of the bond between these atoms, denoted as $\Delta r_{\langle ij \rangle}$, can be expressed in the q coordinates as follows:

$$\Delta r_{\langle ij \rangle} = \frac{1}{r^e_{\langle ij \rangle}} [(x_i^e - x_j^e)(x_i - x_j) + (y_i^e - y_j^e)(y_i - y_j) + (z_i^e - z_j^e)(z_i - z_j)] \tag{10}$$

where superscript "e" denotes an equilibrium quantity. The unnormalized translations and rotations are

$$T_x = \sum_i x_i \tag{11}$$

$$R_x = \sum_i y_i^e z_i - z_i^e y_i \tag{12}$$

and similarly for y and z components. These relations can now be collected in the traditional **B** matrix, which transforms Cartesian displacements into internal and collective coordinates:

$$\mathbf{s} = \mathbf{B}\mathbf{q} \tag{13}$$

$$\mathbf{q} = \mathbf{B}^{-1}\mathbf{s} \tag{14}$$

B is a square matrix, since **s** and **q** have the same dimensions. The group-theoretical relation of eq 4 guarantees **B** to be nonsingular.

We now turn to the vibrational potential energy. Since the vibrational modes span the same symmetry as that of the bond stretches (eq 4), the potential can be written as

$$2V = \sum_{\langle ij \rangle \langle mn \rangle} k_{\langle ij \rangle \langle mn \rangle} \Delta r_{\langle ij \rangle} \Delta r_{\langle mn \rangle} \tag{15}$$

The k's are the force constants and describe a complete force

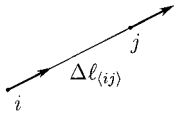

Figure 1. Definition of slides.

field. We follow here a convention where the summation indices $\langle ij \rangle$ and $\langle mn \rangle$ run independently over all bonds. The sum therefore contains e^2 terms, of which at most $e(e+1)/2$ are distinct, but molecular symmetry will usually yield a much smaller set of independent force constants. Their number is equal to the number of copies of the totally symmetric representation Γ_0 contained in the symmetric square of the edge representation $\Gamma_\sigma(e)$.

Nowadays, many ab initio programs provide accurate calculations of the Hessian matrix, from which the internal force constants of our force field can easily be obtained. The Hessian matrix, **H**, defines the potential in Cartesian form, according to

$$2V = \mathbf{q}^\dagger \mathbf{H} \mathbf{q} \tag{16}$$

where the dagger denotes transposition of rows and columns. The elements of **H** may thus be expressed as

$$H_{kl} = \frac{\partial^2 V}{\partial q_k \partial q_l} \tag{17}$$

With the **B** matrix, one can now switch to internal and collective coordinates as follows:

$$2V = \mathbf{s}^\dagger (\mathbf{B}^{-1})^\dagger \mathbf{H} \mathbf{B}^{-1} \mathbf{s} \tag{18}$$

The second-order derivatives for the interaction between two *s* coordinates thus read:

$$\frac{\partial^2 V}{\partial s_a \partial s_b} = \sum_{pq} (B^{-1})_{pa} H_{pq} (B^{-1})_{qb} \tag{19}$$

Derivatives involving collective modes will automatically vanish, as the Hessian is invariant under translations and rotations. In this way, one obtains all $e(e+1)/2$ bond−bond interaction constants. They may easily be sorted into sets of symmetry-equivalent constants. A practical application to the dodecaborane dianion will be illustrated in section 5.1.

4. Complete Force Field for a Trivalent Cage

In a trivalent cage, each atom is connected to three neighbors. According to the symmetry theorem,[1] the Cartesian displacement coordinates are now transformed to $3v/2$ bond stretches, $\Delta r_{\langle ij \rangle}$, and $3v/2$ bond slides, $\Delta \not{r}_{\langle ij \rangle}$. Together, these form the set of internal *s* coordinates of the trivalent cage:

$$\mathbf{s} = \begin{pmatrix} \Delta r_{\langle 12 \rangle} \\ \Delta r_{\langle 13 \rangle} \\ \vdots \\ \Delta \not{r}_{\langle 12 \rangle} \\ \Delta \not{r}_{\langle 13 \rangle} \\ \vdots \end{pmatrix} \tag{20}$$

The expressions for the bond stretches in terms of Cartesian displacement coordinates were given in eq 10 and now appear in the upper half of the **B** matrix. The slides are translations of two atoms along the direction of their common bond, as shown in Figure 1. These type of coordinates have not been used previously in studies of cluster vibrations.

By convention, we define the positive sense of $\Delta \not{r}_{\langle ij \rangle}$ as a translation from atom *i* to atom *j*. Hence, one has

$$\Delta \not{r}_{\langle ji \rangle} = -\Delta \not{r}_{\langle ij \rangle} \tag{21}$$

The slides can easily be expressed in Cartesian displacements of the atoms concerned:

$$\Delta \not{r}_{\langle ij \rangle} = \frac{1}{r^{\mathrm{e}}_{\langle ij \rangle}} [(x_j^{\mathrm{e}} - x_i^{\mathrm{e}})(x_i + x_j) + (y_j^{\mathrm{e}} - y_i^{\mathrm{e}})(y_i + y_j) + (z_j^{\mathrm{e}} - z_i^{\mathrm{e}})(z_i + z_j)] \tag{22}$$

The expressions of this type provide the remaining lower half of the **B** matrix. The potential energy of vibration is given by

$$2V = \sum_{\langle ij \rangle \langle mn \rangle} (k^{rr}_{\langle ij \rangle \langle mn \rangle} \Delta r_{\langle ij \rangle} \Delta r_{\langle mn \rangle} + 2k^{r\not{r}}_{\langle ij \rangle \langle mn \rangle} \Delta r_{\langle ij \rangle} \Delta \not{r}_{\langle mn \rangle} + k^{\not{r}\not{r}}_{\langle ij \rangle \langle mn \rangle} \Delta \not{r}_{\langle ij \rangle} \Delta \not{r}_{\langle mn \rangle}) \tag{23}$$

where we have used $k^{\not{r}r}_{\langle mn \rangle \langle ij \rangle} = k^{r\not{r}}_{\langle ij \rangle \langle mn \rangle}$. In this expression, $\langle ij \rangle$ and $\langle mn \rangle$ run independently over all bonds. Note in particular that constants $k^{r\not{r}}_{\langle ij \rangle \langle mn \rangle}$ and $k^{r\not{r}}_{\langle mn \rangle \langle ij \rangle}$ are not necessarily equal, as exchanging the roles of stretching and sliding bonds may give different contributions to the potential energy.

There are three types of force constants, corresponding to the three possible combinations of stretches and slides. These constants can be extracted directly from the Hessian, following the same procedure as that in the case of the deltahedron, i.e., by a matrix transformation involving the inverse of the **B** matrix, as described in eq 19.

The total number of nonsymmetry related constants in the potential energy expression is equal to the number of times the totally symmetric representation occurs in the symmetrized square of the $\Gamma_\sigma(e) + \Gamma_{||}(e)$ sum representation. This symmetrized square can further be decomposed into three parts:

$$[\Gamma_\sigma(e) + \Gamma_{||}(e)]^2 = [\Gamma_\sigma(e)]^2 + [\Gamma_{||}(e)]^2 + \Gamma_\sigma(e) \times \Gamma_{||}(e) \tag{24}$$

where square brackets denote symmetrized parts. The numbers of the totally symmetric representations in these three parts correspond, respectively, to the numbers of nonsymmetry related constants of type k^{rr}, $k^{\not{r}\not{r}}$, and $k^{r\not{r}}$.

The force field which is obtained in this way is, however, not free from redundancies. The external collective modes contained in the mechanical representation give rise to a set of redundancy conditions between the force constants, which can easily be derived by requiring that the forces associated with the spurious modes be zero. First, consider the translations. A translation in the *x* direction induces slides of all bonds that have a component along this direction. This is expressed by a total differential of the following type:

$$\frac{\mathrm{d}}{\mathrm{d}T_x} = 2 \sum_{\langle ab \rangle} \frac{x_b^{\mathrm{e}} - x_a^{\mathrm{e}}}{r^{\mathrm{e}}_{\langle ab \rangle}} \frac{\partial}{\partial \Delta \not{r}_{\langle ab \rangle}} \tag{25}$$

and similarly for T_y and T_z. The associated force is given by

$$\frac{\mathrm{d}V}{\mathrm{d}T_x} = 2 \sum_{\langle ab \rangle} \sum_{\langle ij \rangle} \frac{x_b^{\mathrm{e}} - x_a^{\mathrm{e}}}{r^{\mathrm{e}}_{\langle ab \rangle}} (k^{r\not{r}}_{\langle ij \rangle \langle ab \rangle} \Delta r_{\langle ij \rangle} + k^{\not{r}\not{r}}_{\langle ij \rangle \langle ab \rangle} \Delta \not{r}_{\langle ij \rangle}) \tag{26}$$

This force will be zero if the following redundancy relations

are fulfilled:

$$\sum_{\langle ab\rangle} \frac{x_b^e - x_a^e}{r_{\langle ab\rangle}^e} k_{\langle ij\rangle\langle ab\rangle}^{r/} = 0 \tag{27}$$

$$\sum_{\langle ab\rangle} \frac{x_b^e - x_a^e}{r_{\langle ab\rangle}^e} k_{\langle ij\rangle\langle ab\rangle}^{//} = 0 \tag{28}$$

and similarly for *y* and *z* components.

The rotations can be treated in an analogous way. Again, an overall rotation does not affect the bond lengths and therefore cannot interfere with stretches, but it may induce slides. The total differential for a rotation about the *z* axis is given by

$$\frac{d}{dR_z} = 2\sum_{\langle ab\rangle} \frac{x_a^e y_b^e - x_b^e y_a^e}{r_{\langle ab\rangle}^e} \frac{\partial}{\partial \Delta_{\langle ab\rangle}^{/}} \tag{29}$$

and similarly for R_x and R_y. The associated force is

$$\frac{dV}{dR_z} = 2\sum_{\langle ab\rangle}\sum_{\langle ij\rangle} \frac{x_a^e y_b^e - x_b^e y_a^e}{r_{\langle ab\rangle}^e} (k_{\langle ij\rangle\langle ab\rangle}^{r/} \Delta r_{\langle ij\rangle} + k_{\langle ij\rangle\langle ab\rangle}^{//} \Delta_{\langle ij\rangle}^{/}) \tag{30}$$

This force vanishes under the additional redundancy conditions:

$$\sum_{\langle ab\rangle} \frac{x_a^e y_b^e - x_b^e y_a^e}{r_{\langle ab\rangle}^e} k_{\langle ij\rangle\langle ab\rangle}^{r/} = 0 \tag{31}$$

$$\sum_{\langle ab\rangle} \frac{x_a^e y_b^e - x_b^e y_a^e}{r_{\langle ab\rangle}^e} k_{\langle ij\rangle\langle ab\rangle}^{//} = 0 \tag{32}$$

and similarly for the *x* and *y* components.

For each bond $\langle ij\rangle$, we thus have in principle 12 redundancy conditions, or 12*e* conditions in total. This number will, of course, also be drastically reduced whenever symmetry is present, as will be illustrated in section 5.2 for the example of cubane.

5. Applications

5.1. Dodecaborane, $B_{12}H_{12}^{2-}$. The largest closo-borane anion, $B_{12}H_{12}^{2-}$ exists as a near-perfect icosahedron in its salts, invariably distorted slightly by steric hindrance with the surrounding lattice.[8] Ab initio calculations of the vibrational frequencies in a 4-31G basis were performed by Brint et al. as part of a wider study of theoretical and experimental IR and Raman spectra of boranes.[9,10] We have recalculated the spectrum with the DGauss density functional program,[11] which is included in the UniChem package.[12] Different functionals were investigated, the GGA BLYP with DZVP2 global orbital basis set yielding results which were closest to experimental frequencies. In Table 1, we collect experimental and theoretical geometries and vibrational spectra. The experimental IR and Raman spectra refer to solid salts of, respectively, $Na_2B_{12}H_{12}$ [13] and $K_2B_{12}H_{12}$.[14] Equivalent data for the deuterated salts are also available.

The experimental pattern is reproduced quite accurately by the ab initio results. As expected, SCF frequencies overestimate the experimental values, especially for the high-energy ν_{B-H} stretching modes above 2000 cm^{-1}, with discrepancies of up to 7%. In this respect, the DFT results score slightly better.

TABLE 1: Spectroscopic and Geometrical Data for $B_{12}H_{12}^{2-}$

label	$\bar{\nu}_{exp}$ [13,14] (cm^{-1})	$\bar{\nu}_{calc}$ [a] (cm^{-1})	$\bar{\nu}_{calc}$ [b] (cm^{-1})
A_g	2517	2687	2540
	745	741	725
T_{1g}		1064	923
T_{1u}	2480	2642	2504
	1070	1155	1026
	720	720	683
T_{2u}		2611	2476
		809	732
G_g		1035	900
		696	631
G_u		945	822
		774	717
H_g	2470	2618	2483
	955	1013	891
	770	792	728
	580	600	558
H_u		1043	911
		526	499
bond	(Å)[8]	(Å)	(Å)
⟨B−B⟩	1.77	−	1.804
⟨B−H⟩	1.07	−	1.206

[a] HF-SCF calculation, 4-31G basis.[9,10] [b] DFT calculation, DGauss,[11] BLYP-DZVP2.

The normal modes of the B_{12} cage were treated analytically in earlier papers by Weber and Thorpe[15] and Boyle and Parker,[6] using simplified force field models. A crucial problem in the extraction of force field parameters, which also appears in applying the present complete field method, concerns the correct assignment of modes with predominant skeletal character. Indeed, except for the ν_{B-H} stretches, the ν_{B-B} vibrations of the cluster cage and the δ_{B-B-H} bending modes of the external hydrogens may show substantial mixing. Muetterties et al.[13] assigned the lowest IR and Raman frequencies, at 745 (A_g), 720 (T_{1u}), 580 (H_g), and 770 (H_g) cm^{-1}, to skeletal modes. Abdul-Fattah and Butler[16] later reversed the assignment of the T_{1u} modes, claiming a predominant ν_{B-B} character for the middle-frequency 1070 cm^{-1} mode versus a δ_{B-B-H} assignment for the 720 cm^{-1} mode. Only a full calculation of the total Hessian can settle this question unambiguously.

To obtain a complete force field for the oscillating icosahedral cage, we must first separate cluster vibrations from the motions of the exohedral hydrogen atoms. The separation procedure is described in appendix A. The effective cluster vibrations are obtained by projecting out the modes for which the hydrogen atoms follow the boron displacements adiabatically. The resulting effective Hessian, $\mathbf{H}_{eff}$ for the skeletal displacements of the boron atoms, is given by

$$\mathbf{H}_{eff} = \mathbf{H}^{BB} - \mathbf{H}^{BH}(\mathbf{H}^{HH})^{-1}\mathbf{H}^{HB} \tag{33}$$

where $\mathbf{H}^{BB}$ and $\mathbf{H}^{HH}$ are, respectively, the diagonal boron−boron and hydrogen−hydrogen blocks of the Hessian, and $\mathbf{H}^{BH}$ and $\mathbf{H}^{HB}$ are the corresponding off-diagonal blocks. To this effective potential matrix is associated an effective mass matrix, **M**:

$$\mathbf{M} = m_B\mathbf{I} + m_H\mathbf{H}^{BH}(\mathbf{H}^{HH})^{-1}(\mathbf{H}^{HH})^{-1}\mathbf{H}^{HB} \tag{34}$$

where m_B and m_H are the masses of, respectively, boron and hydrogen atoms. The frequencies ν of the effective modes are then obtained by solving the eigenvalue problem:

$$|\mathbf{H}_{\text{eff}} - 4\pi^2\nu^2\mathbf{M}| = 0 \tag{35}$$

where ν are the frequencies in Hz; the elements of $\mathbf{H}_{\text{eff}}$ are in N/m, and those of $\mathbf{M}$ in kg.

From the DFT results, we have calculated the effective Hessian and mass matrix and diagonalized the resulting matrix equation. The frequencies (in cm^{-1}) are given in Table 2, labeled $\bar{\nu}_{\text{eff}}$.

When comparing these frequencies with the experimental and calculated spectra in Table 1, it is clearly seen that effective cluster modes are always very close to the lowest eigenmodes of each symmetry type.

The effective potential for the skeletal modes is now decomposed over all bond−bond interactions, according to the general group-theoretical result:

$$\begin{aligned} 2V_{\text{eff}} &= \mathbf{q}^{\text{B}\dagger}\mathbf{H}_{\text{eff}}\mathbf{q}^{\text{B}} \\ &= k_1 \sum_{\langle ij\rangle=1}^{30} (\Delta r_{\langle ij\rangle})^2 + k_2 \sum_{D_2}^{120} \Delta r_{\langle ij\rangle}\Delta r_{\langle im\rangle} + \\ & k_3 \sum_{D_3}^{120} \Delta r_{\langle ij\rangle}\Delta r\langle_{ik}\rangle + k_4 \sum_{D_4}^{120} \Delta r_{\langle ij\rangle}\Delta r_{\langle km\rangle} + k_5 \sum_{D_5}^{120} \Delta r_{\langle ij\rangle}\Delta r_{\langle lm\rangle} + \\ & k_6 \sum_{D_6}^{120} \Delta r_{\langle ij\rangle}\Delta r_{\langle kl\rangle} + k_7 \sum_{D_7}^{120} \Delta r_{\langle ij\rangle}\Delta r_{\langle kn\rangle} + k_8 \sum_{D_8}^{120} \Delta r_{\langle ij\rangle}\Delta r_{\langle ln\rangle} + \\ & k_9 \sum_{D_9}^{30} \Delta r_{\langle ij\rangle}\Delta r_{\langle no\rangle} \end{aligned} \tag{36}$$

The bond indices in this expression refer to the labeling system, shown in Figure 2. The summation domains D_x indicate that both bond indices in a sum run independently over all pairs of given type. As an example, k_2 is the interaction constant between stretchings of two adjacent bonds. Since each of the 30 $\langle ij\rangle$ bonds has four $\langle im\rangle$ nearest neighbors, the summation domain D_2 contains 120 combinations. Note that there are, in total, 465 permutationally distinct bond−bond combinations, but only 9 independent force constants. This number is equal to the number of times the A_g representation is contained in the symmetric square of Γ_{vib} for the skeletal modes, with

$$\Gamma_{\text{vib}}(B_{12}) = A_g + T_{1u} + T_{2u} + G_g + G_u + 2H_g + H_u \tag{37}$$

In contrast, only eight frequencies are experimentally observable. The ninth experimental parameter is associated with the eigenvector composition of the H_g modes. Indeed, since there are two H_g modes in an icosahedral cage, their eigenvector composition represents an extra degree of freedom which does not depend on symmetry. In principle, observables such as intensities or isotope shifts can be used to extract this parameter from experiment, thus yielding enough empirical data to match the complete force model.

The complete set of force constants can now easily be calculated from the effective Hessian by taking the appropriate second derivatives. The results are displayed in Table 3.

The small deviations in the calculated values are due to slight numerical instabilities in the DGauss program, which does not make use of the icosahedral point group symmetry.

Figure 2 shows a "magnitude diagram" of the boron skeleton. The line thickness and colouring varies according to the magnitude of the constant between the central bond $\langle ij\rangle$ and the bond considered.

TABLE 2: Frequencies for the B_{12} Cage from the Effective Hessian

label	$\bar{\nu}_{\text{eff}}$ [a] (cm^{-1})	$\bar{\nu}_{A_{12}}$ [b] (cm^{-1})
A_g	728	727
T_{1u}	763	782
T_{2u}	733	728
G_g	664	658
G_u	745	735
H_g	825	821
	562	553
H_u	508	505

[a] $\bar{\nu}_{\text{eff}}$ refers to the eigenvalues of the effective Hessian (eq 33) with the appropriate mass matrix (eq 34). [b] $\bar{\nu}_{A_{12}}$ refers to the eigenvalues of the effective Hessian for a cage of BH superatoms with a mass $m_{\text{BH}} = 11.819$ au.

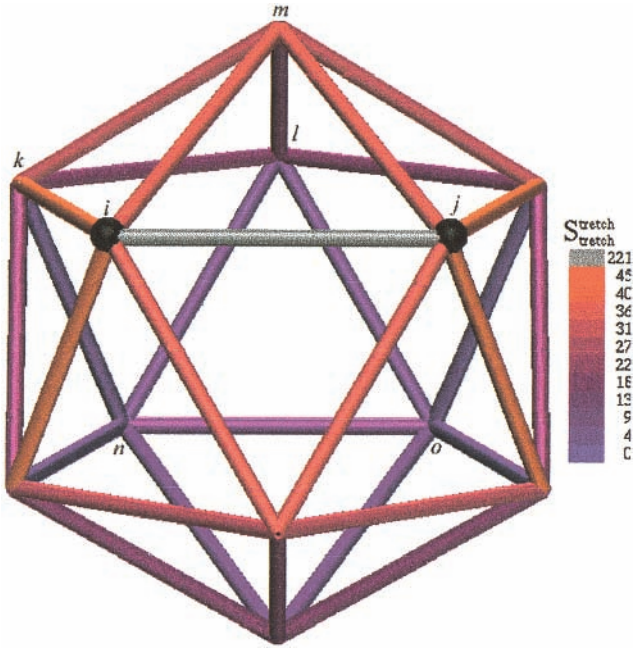

Figure 2. "Magnitude diagram" of the boron skeleton in dodecaborane. Bond indices are associated with summation domains of eq 36. Vertex *m* shares a face with $\langle ij\rangle$, vertex *k* only an edge, vertex *l* is at distance 2 from both *i* and *j*, and vertexes *n* and *o* are at distances 2 and 3 from *i* (3 and 2 from *j*). The gray bond, between the black atoms, is the central bond $\langle ij\rangle$; the color of this bond is not drawn to scale because the self-interaction of this bond is about 5 times larger than the second largest interaction.

TABLE 3: Force Constants for B_{12}, in N/m

constant		value[a]	value[b]	σ [c]
k_1	$\langle ij\rangle\langle ij\rangle$	352	221.48	0.8%
k_2	$\langle ij\rangle\langle im\rangle$	−109	−33.12	2.8%
k_3	$\langle ij\rangle\langle ik\rangle$	54	41.46	1.4%
k_4	$\langle ij\rangle\langle km\rangle$	0	−29.57	2.1%
k_5	$\langle ij\rangle\langle lm\rangle$	0	−17.36	1.3%
k_6	$\langle ij\rangle\langle kl\rangle$	0	17.56	1.6%
k_7	$\langle ij\rangle\langle kn\rangle$	0	0.88	31.4%
k_8	$\langle ij\rangle\langle ln\rangle$	0	−3.95	5.4%
k_9	$\langle ij\rangle\langle no\rangle$	0	8.06	3.1%

[a] Eq 36, with $k_4 - k_9$ zero, fitted to $\bar{\nu}_{A_{12}}$ from Table 2. [b] Calculated from the effective Hessian. [c] Standard deviation.

This figure shows that interaction between bonds in general decreases with their distance; however, e.g., transversal interactions of the $\langle ij\rangle - \langle no\rangle$ type are much stronger than those of the $\langle ij\rangle - \langle kn\rangle$ type.

Figure 3 shows the "sign distribution" of the interactions on the boron skeleton. This reflects whether a bond tends to shrink ("+" sign) as the main bond stretches or tends to stretch also ("−" sign).

We have also derived closed form expressions for the frequencies of a 12-atom icosahedron as a function of the nine force constants:

$$A_g:\ m\omega_1^2 = 2(3-\Phi)(k_1 + 4k_2 + 4k_3 + 4k_4 + 4k_5 + 4k_6 + 4k_7 + 4k_8 + k_9) \quad (38)$$

$$T_{1u}:\ m\omega_2^2 = 3(k_1 + 2\Phi k_2 + 2k_3 + 2\Phi^{-1}k_4 - 2\Phi^{-1}k_6 - 2k_7 - 2\Phi k_8 - k_9) \quad (39)$$

$$T_{2u}:\ m\omega_3^2 = 2(-\Phi+2)(k_1 - 2\Phi^{-1}k_2 + 2k_3 - 2\Phi k_4 + 2\Phi k_6 - 2k_7 + 2\Phi^{-1}k_8 - k_9) \quad (40)$$

$$G_g:\ m\omega_4^2 = \frac{\Phi+2}{2}(k_1 - k_2 - k_3 - k_4 + 4k_5 - k_6 - k_7 - k_8 + k_9) \quad (41)$$

$$G_u:\ m\omega_5^2 = \frac{3\Phi+2}{2}(k_1 + k_2 - 3k_3 - k_4 + k_6 + 3k_7 - k_8 - k_9) \quad (42)$$

$$H_g:\ m\omega_6^2 + m\omega_7^2 = 4k_1 + 2(\Phi+1)k_2 - 2(2\Phi-1)k_3 + 2(\Phi-2)k_4 - 8k_5 + 2(\Phi-2)k_6 - 2(2\Phi-1)k_7 + 2(\Phi+1)k_8 + 4k_9 \quad (43)$$

$$m^2\omega_6^2\,\omega_7^2 = 8\left[\frac{1}{4}k_1^2 - k_1k_5 + \frac{1}{2}k_1k_9 - k_2^2 + k_2k_3 + k_2k_4 + k_2k_6 + k_2k_7 - 2k_2k_8 - k_3^2 + k_3k_4 + k_3k_6 - 2k_3k_7 + k_3k_8 - k_4^2 - 2k_4k_6 + k_4k_7 + k_4k_8 + k_5^2 - k_5k_9 - k_6^2 + k_6k_7 + k_6k_8 - k_7^2 + k_7k_8 - k_8^2 + \frac{1}{4}k_9^2\right] \quad (44)$$

$$H_u:\ m\omega_8^2 = k_1 - 2k_2 + 2k_4 - 2k_6 + 2k_8 - k_9 \quad (45)$$

Here, $\omega = 2\pi\nu$ is the angular frequency, m is the mass of the B−H cluster superatom, and Φ is the "golden number", $^1/_2(1 + \sqrt{5})$. Frequencies calculated with these expressions are displayed in the Table 2, labeled $\bar{\nu}_{A_{12}}$. They are very close to the results of the effective cluster Hamiltonian, which implies that the effective mass matrix is approximately equal to $(m_B + m_H)\mathbf{I}$.

We may now compare these results with the previous analysis of Boyle and Parker,[6] who only took into account interactions between neighboring bonds, as described by the first three force constants. (The actual force constant expressions in ref 6 contain errors, due to a few wrong matrix elements in the matrix transformation between internal coordinates and symmetry coordinates. The correct expressions can be obtained from our eq 36 by putting k_4−k_9 equal to zero.) The results in the table clearly show that this approximation overlooks the important contribution from the next three force constants, k_4, k_5, and k_6, which concern pairs of nonadjacent bonds.

5.2. Cubane, C_8H_8. The cubane molecule was first synthesized in 1964,[17] and its regular geometry was soon confirmed by X-ray diffraction.[18] The high symmetry and unusual geometry of the molecule make it an interesting candidate for spectroscopic investigations. Several IR and Raman[19,20] studies have been published, of which the most complete presents a full set of fundamental frequencies with a suggested assignment. The IR spectrum of cubane is very simple, as only the T_{1u} fundamental vibrations appear. Three lines are observed in the IR spectrum, which is the number expected for a C_8H_8 molecule possessing O_h symmetry.

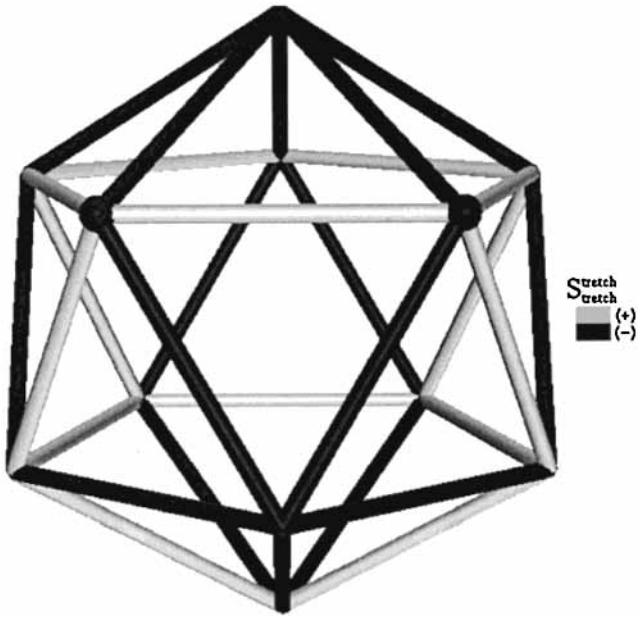

Figure 3. "Sign distribution" of the stretch interactions in the boron skeleton ($\langle ij \rangle$ is situated between the two black atoms).

TABLE 4: Spectroscopic and Geometrical Data for C_8H_8

label	$\bar{\nu}_{exp}$ [18−20] (cm^{-1})	$\bar{\nu}_{calc}$ [a] (cm^{-1})
A_{1g}	2995	3193
	1002	1013
A_{2u}	2987	3137
	839	1069
E_g	1083	1119
	912	928
E_u	1151	1203
	617	624
T_{1g}	1130	1177
T_{1u}	2978	3164
	1230	1263
	853	866
T_{2g}	2970	3151
	1182	1226
	821	835
	665	704
T_{2u}	1036	1080
	829	850
bond	(Å)	(Å)
⟨C−C⟩	1.55	1.589
⟨C−H⟩	1.10	1.089

[a] DFT calculation, Gaussian,[25] B3LYP-d95.

A number of theoretical studies[21−24] of the geometry and vibrational structure, at different levels of calculation, have appeared since cubane was synthesized. The geometries calculated in these studies compare reasonably well with experiment. We repeated calculations of the geometry and the vibrational spectrum with Gaussian[25] (Dunning/Huzinaga full double zeta basis set[26] with Becke's three-parameter hybrid method using the LYP correlation functional[27]). A comparison of experimental and calculated geometries and frequencies is presented in Table 4.

As for the boron cage (vide supra), the effective skeletal modes for the carbon cage were projected out using the method explained in the appendix. The resulting matrix equation was

TABLE 5: Frequencies for the C_8 Cage from the Effective Hessian

label	$\bar{\nu}_{\text{eff}}$ [a] (cm^{-1})	$\bar{\nu}_{A_8}$ [b] (cm^{-1})	label	$\bar{\nu}_{\text{eff}}$ [a] (cm^{-1})	$\bar{\nu}_{A_8}$ [b] (cm^{-1})
A_{1g}	1017	1018	T_{1u}	948	974
A_{2u}	1074	1068	T_{2g}	935	953
E_g	1020	996	T_{2g}	717	717
E_u	653	687	T_{2u}	919	937

[a] $\bar{\nu}_{\text{eff}}$ refers to the eigenvalues of the effective Hessian (eq 33) with the appropriate mass matrix (eq 34). [b] $\bar{\nu}_{A_8}$ refers to the eigenvalues of the effective Hessian for a cage of CH superatoms with a mass $m_{CH} = 13.019$ u.

TABLE 6: Bond−Bond Interactions for C_8

$k^{rr}_{\langle ij\rangle\langle ij\rangle} = K^r_0$	$k^{ll}_{\langle ij\rangle\langle ij\rangle} = K^l_0$	diagonal element
$k^{rr}_{\langle ij\rangle\langle ik\rangle} = K^r_{1\perp}$	$k^{ll}_{\langle ij\rangle\langle ik\rangle} = K^l_{1\perp}$	nearest perpendicular
$k^{rr}_{\langle ij\rangle\langle mn\rangle} = K^r_{1\|\|}$	$k^{ll}_{\langle ij\rangle\langle \cdot mn\rangle} = K^l_{1\|\|}$	nearest parallel
$k^{rr}_{\langle ij\rangle\langle lo\rangle} = K^r_{2\perp}$	$k^{ll}_{\langle ij\rangle\langle lo\rangle} = K^l_{2\perp}$	next nearest perpendicular
$k^{rr}_{\langle ij\rangle\langle op\rangle} = K^r_{2\|\|}$	$k^{ll}_{\langle ij\rangle\langle op\rangle} = K^l_{2\|\|}$	next nearest parallel
$k^{rl}_{\langle ij\rangle\langle ik\rangle} = K^{rl}_1$		stretch($\langle ij\rangle$)-slide($\langle ik\rangle$)
$k^{rl}_{\langle ij\rangle\langle lo\rangle} = K^{rl}_2$		stretch($\langle ij\rangle$)-slide($\langle lo\rangle$)

diagonalized to obtain frequencies; they are listed in Table 5, labeled $\bar{\nu}_{\text{eff}}$. As opposed to the boron cage, the lowest frequency modes are not always of predominant skeletal type. As an example, the skeletal E_g and T_{2u} modes are to be convolutions of low- and high-frequency eigenmodes of cubane.

The stretching and sliding components of the mechanical representation for a regular cube are given by

$$\Gamma_o(e) = A_{1g} + E_g + T_{1u} + T_{2g} + T_{2u} \tag{46}$$

$$\Gamma_{||}(e) = A_{2u} + E_u + T_{1g} + T_{1u} + T_{2g} \tag{47}$$

The complete force field will thus contain 12 force constants: five for the stretching modes, five for the slidings, and two for the interactions between equisymmetric stretchings and slidings. The different bond−bond interactions are summarized in Table 6.

The bond indices in these expressions refer to the labeling system shown in Figure 4.

Using this new notation, the effective potential can be written as

$$\begin{aligned}2V_{\text{eff}} = {} & K^r_0\sum_{D_1}^{12}(\Delta r_{\langle ij\rangle})^2 + K'_0\sum_{D_1}^{12}(\Delta'_{\langle ij\rangle})^2 + K^r_{1\perp}\sum_{D_2}^{48}\Delta r_{\langle ij\rangle}\Delta r_{\langle ik\rangle} + \\ & K'_{1\perp}\sum_{D_2}^{48}\Delta'_{\langle ij\rangle}\Delta'_{\langle ik\rangle} + K^r_{1||}\sum_{D_3}^{24}\Delta r_{\langle ij\rangle}\Delta r_{\langle mn\rangle} + K'_{1||}\sum_{D_3}^{24}\Delta'_{\langle ij\rangle}\Delta'_{\langle mn\rangle} + \\ & K^r_{2\perp}\sum_{D_4}^{48}\Delta r_{\langle ij\rangle}\Delta r_{\langle lo\rangle} + K'_{2\perp}\sum_{D_4}^{48}\Delta'_{\langle ij\rangle}\Delta'_{\langle lo\rangle} + K^r_{2||}\sum_{D_5}^{12}\Delta r_{\langle ij\rangle}\Delta r_{\langle op\rangle} + \\ & K'_{2||}\sum_{D_5}^{12}\Delta'_{\langle ij\rangle}\Delta'_{\langle op\rangle} + K^{r'}_1\sum_{D_6}^{48}\Delta r_{\langle ij\rangle}\Delta'_{\langle ik\rangle} + K^{r'}_2\sum_{D_7}^{48}\Delta r_{\langle ij\rangle}\Delta'_{\langle lo\rangle}\end{aligned} \tag{48}$$

The complete set of force constants was calculated from the effective Hessian; the results are displayed in Table 7. Note that the definitions of K' and $K^{r'}$ constants imply specific directions of the bonds concerned. This is not the case for the K^r constants, since no direction is involved in a stretch. The signs in Table 7 refer to the interactions between the bonds used in the definitions for the K constants in Table 6 and to the geometry given in Figure 4, where the "positive slide" direction

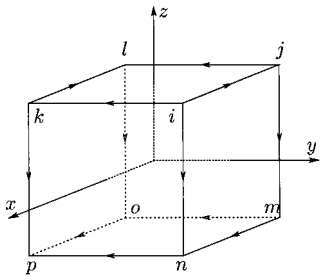

Figure 4. Bond indices associated with force constants notation, introduced in Table 6. "Positive slide directions" are also indicated.

TABLE 7: Force Constants for C_8, in N/m

constant	value	constant	value
K^r_0	358.22	$K^l_{1\perp}$	46.01
$K^r_{1\perp}$	4.81	$K^l_{1||}$	66.71
$K^r_{1||}$	10.01	$K^l_{2\perp}$	−3.65
$K^r_{2\perp}$	−2.01	$K^l_{2||}$	−16.56
$K^r_{2||}$	8.13	K^{rl}_1	3.21
K^l_0	116.86	K^{rl}_2	−3.21

is indicated. To calculate the potential using eq 46, the signs must be adjusted according to the bond pair considered.

Using the determined force constants, we can calculate frequencies for the cubane cage, consisting of CH oscillators with mass $m_C + m_H$. The results are listed in Table 5, labeled $\bar{\nu}_{A_8}$, and comply with the following expressions:

$$A_{1g}: \quad m\omega_1^2 = 2(K^r_0 + 4K^r_{1\perp} + 2K^r_{1||} + 4K^r_{2\perp} + K^r_{2||}) \tag{49}$$

$$A_{2u}: \quad m\omega_2^2 = 2(K'_0 + 4K'_{1\perp} + 2K'_{1||} + 4K'_{2\perp} - K'_{2||}) \tag{50}$$

$$E_g: \quad m\omega_3^2 = 2(K^r_0 - 2K^r_{1\perp} + 2K^r_{1||} - 2K^r_{2\perp} + K^r_{2||}) \tag{51}$$

$$E_u: \quad m\omega_4^2 = 2(K'_0 - 2K'_{1\perp} + 2K'_{1||} - 2K'_{2\perp} - K'_{2||}) \tag{52}$$

$$T_{1u}: \quad m\omega_5^2 = 2(K^r_0 + 2K^r_{1\perp} - 2K^r_{2\perp} - K^r_{2||}) \tag{53}$$

$$T_{2g}: \quad m\omega_6^2 + m\omega_7^2 = 2(K^r_0 - 2K^r_{1||} + K^r_{2||} + K'_0 + 2K'_{1\perp} - 2K'_{2\perp} + K'_{2||}) \tag{54}$$

$$m^2\omega_6^2\,\omega_7^2 = 4(K^r_0 - 2K^r_{1||} + K^r_{2||})(K'_0 + 2K'_{1\perp} - 2K'_{2\perp} + K'_{2||}) - 32(K^{r\prime}_1 - K^r_2)^2 \tag{55}$$

$$T_{2u}: \quad m\omega_8^2 = 2(K^r_0 - 2K^r_{1\perp} + 2K^r_{2\perp} - K^r_{2||}) \tag{56}$$

As noted previously for the boron cage, these frequencies match the results of the effective Hessian calculations.

As mentioned in section 4, there are several redundancy conditions to be fulfilled (see eqs 27, 28, 31, and 32), giving rise to 144 conditions in total. However, inspection shows that only three independent conditions remain:

$$K'_0 - 2K'_{1||} - K'_{2||} = 0 \tag{57}$$

$$K^{r\prime}_1 + K^{r\prime}_2 = 0 \tag{58}$$

$$K'_0 - 2K'_{1\perp} + 2K'_{2\perp} + K'_{2||} = 0 \tag{59}$$

These equations indicate that the translations (eq 57) and rotations (eq 59) are spurious modes and that the translation does not interact with the T_{1u} stretching vibration (eq 58). The

constants from Table 7 satisfy these conditions within the numerical accuracy of the calculation. In this way, only nine independent force constants remain, exactly the number of times the A_{1g} representation occurs in the symmetric square of the representation of the vibrational modes.

5.3. Buckminsterfullerene, C_{60}. Ever since its discovery in 1985 by Kroto et al.,[28] the C_{60} molecule has been the subject of many research projects. The most famous isomer is undoubtedly the so-called "Bucky Ball", where all pentagons are isolated. This molecule has the shape of a truncated icosahedron.

There have been a number of reported measurements of the vibrational transitions in C_{60}.[29−34] There are a total of 46 fundamental vibrational modes for C_{60}, but due to the high symmetry (I_h), there are only four infrared active modes of T_{1u} symmetry and 10 Raman active modes, two of A_g symmetry and eight of H_g symmetry. The remaining 32 modes are silent as fundamental transitions and can only be observed as weak combination bands[34,35] or from inelastic neutron scattering measurements[30] where the selection rules are relaxed.

There have also been a number of theoretical studies[36] of the vibrational modes of C_{60}. Dixon et al.[37] calculated the harmonic vibrational frequencies at the local density functional level by using analytic second derivatives. The calculated values for the observed infrared and Raman transitions are in good agreement with the experimental values, as shown in Table 8.

In addition, several local force fields have been proposed,[39−42] and it has been demonstrated that, to a good approximation, C_{60} vibrates as a thin spherical shell.[41]

5.3.1. Partial Force Field. In earlier work,[41] attempts were made to calculate the vibrational spectrum of C_{60} using an extended Wu force field, containing six force constants. We have now extended this to up to 10 force constants, c_1-c_{10}. The associated potential energy is

$$2V = c_1\sum_{30}(\Delta r_h)^2 + c_2\sum_{60}(\Delta r_p)^2 + c_3 r_p r_h \sum_{120}(\Delta\alpha_h)^2 + c_4 r_p r'_p \sum_{60}(\Delta\alpha_p)^2 + 2c_5\sum_{120}\Delta r_p \Delta r_h + 2c_6\sum_{60}\Delta r_p \Delta r'_p + 2c_7 r_p\sqrt{r_h r'_p}\sum_{120}\Delta\alpha_p\Delta\alpha_h + 2c_8 r_h\sqrt{r_p r'_p}\sum_{60}\Delta\alpha_h\Delta\alpha'_h + 2c_9\sum_{60}(\Delta R_p)^2 + 2c_{10}\sum_{120}(\Delta R_h)^2 \quad (60)$$

The parameters, used in this expression, refer to the pentagon−hexagon bond system as shown in Figure 5.

Constants c_7 and c_8 were added to complete the force field of nearest neighbors. They offer a description of the pyramidalization of the carbon atoms. Constants c_9 and c_{10} introduce additional springs between atoms that are second neighbors. Their main effect is to improve the frequency fit for the lowest H_g squashing mode. This force field describes all potential energy effects caused by changes in bond lengths and angles between neighboring atoms. Values for the 10 force constants, which were optimized in order to obtain a least square fit of calculated frequencies to IR and Raman data, are listed in Table 9; frequencies calculated with these constants are listed in Table 8.

Although the frequencies from this 10-parameter force field are in fairly good agreement with experimental data, the lowest H_g mode at approximately 273 cm^{-1} is still not well reproduced. In the original six-parameter model,[41] this frequency was calculated too low at 214 cm^{-1}. By addition of the local pyramidalization constants c_7 and c_8, the error became even larger, with a calculated value of 207 cm^{-1}. A real improvement, to a value of 245 cm^{-1}, could only be achieved by adding interactions between atoms which are more than one bond away, as expressed by the constants c_9 and c_{10}. This indicates that the

TABLE 8: Spectroscopic and Geometrical Data for C_{60}

label	$\bar{\nu}_{exp}$ [34] (cm^{-1})	$\bar{\nu}_{calc}$ [a] (cm^{-1})	$\bar{\nu}_{calc}$ [b] (cm^{-1})	$\bar{\nu}_{calc}$ [c] (cm^{-1})
A_g	1470	1525	1456.8	1525
	495	499	503.4	499
A_u		972	1080.3	967
T_{1g}		1318	1300.5	1317
		830	889.7	831
		579	583.0	579
T_{2g}	1360	1393	1371.3	1392
		839	978.9	839
		804	814.3	805
	566	551	567.4	549
T_{1u}	1429	1486	1445.3	1485
	1183	1224	1160.4	1224
	576	591	599.2	591
	526	535	542.3	535
T_{2u}		1571	1522.4	1570
	1201	1234	1190.7	1233
	1026	996	1016.2	995
		726	734.6	726
	356	342	344.6	342
G_g	1524	1548	1517.4	1547
	1356	1347	1368.9	1347
	1076	1122	1086.3	1123
		788	860.8	785
		573	545.2	571
	486	484	445.7	484
G_u	1446	1480	1474.8	1480
	1310	1359	1337.2	1358
	970	984	961.0	981
		830	926.4	829
	760	762	763.3	759
		350	339.8	348
H_g	1578	1618	1560.3	1617
	1426	1475	1447.6	1474
	1251	1297	1222.6	1296
	1101	1128	1135.9	1127
	775	788	774.4	791
	711	727	722.9	727
	432	431	424.3	431
	273	261	245.3	263
H_u	1559	1611	1558.8	1611
	1385	1389	1367.5	1388
		1248	1225.1	1248
		762	830.9	763
		671	666.7	672
		541	510.1	541
		401	350.8	405
bond	(Å)[38]	(Å)	(Å)	(Å)
⟨C−C⟩	1.467	1.445	1.445	1.445
⟨C=C⟩	1.355	1.395	1.395	1.395

[a] DFT.[37] [b] Extended Wu force field. [c] Complete force field.

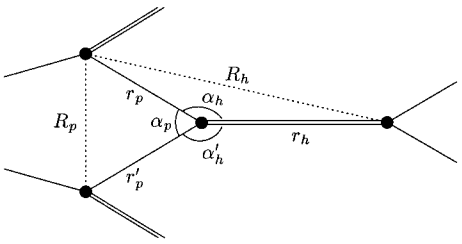

Figure 5. Parameters used in extended Wu force field.

TABLE 9: Force Constants for Extended Wu Force Field (N/m)

c_1	520.1	c_6	9.8
c_2	348.1	c_7	35.1
c_3	68.4	c_8	21.7
c_4	77.6	c_9	42.7
c_5	28.0	c_{10}	11.6

lowest H_g mode, which is important in Jahn−Teller distortions of C_{60} anions,[43] has a strong non-local character. It is associated with an amplitude which varies slowly over the surface of the cluster, and thus is susceptible to long-range interactions.

5.3.2. Complete Force Field. As a basis for the complete force field, we have used the full ab initio Hessian, calculated by Dixon et al.[37] All 160 force constants for the complete force field, as in eq 23, were extracted. Since the DGauss program does not make use of icosahedral symmetry, the resulting force constants for equivalent interactions show slight deviations. If we remove numerical noise by replacing equivalent constants by their mean values and then invert the Hessian problem, frequencies which show precise icosahedral degeneracies are obtained. The results of this symmetry cleaning of the Dixon calculation are also listed in Table 8.

Figure 6 shows a Schlegel diagram with the labeling system for atoms in C_{60}.[44] These labels are used to define the force constants for all types of interactions between two given bonds.

Table 10 lists all values for these force constants and their numerical standard deviation, as obtained from the Hessian in ref 37 before symmetry cleaning. For each force constant, only one of the equivalent pairs is given; the signs in the table refer to these exemplary pairs. The stretch and slide representations for C_{60} are given by

$$\Gamma_\sigma(e) = 2A_g + T_{1g} + 3T_{1u} + T_{2g} + 3T_{2u} + 3G_g + 3G_u + 5H_g + 3H_u \quad (61)$$

$$\Gamma_{||}(e) = A_u + 3T_{1g} + 2T_{1u} + 3T_{2g} + 2T_{2u} + 3G_g + 3G_u + 3H_g + 4H_u \quad (62)$$

Taking the symmetrized squares, we note that the numbers of independent stretch, slide, and stretch−slide interaction constants are, respectively, 50, 47, and 63, in agreement with Table 10.

Several constants turn out to be extremely small, and these cases are always accompanied by high numerical inaccuracies.

The values for the force constants show that the interaction between two bonds decreases with the distance; however, the contributions from the "long-distance interactions" provide essential corrections, since there are many more of them; without these terms, it is very difficult to reproduce all frequencies accurately. The effect of slide−slide interactions decays less rapidly with distance than stretch−stretch interactions.

Considering the relative importance of interactions, the main interactions with a given bond are found on the bonds of the "neighboring rings", i.e., the rings which encircle that bond. Additional interactions, which are still significant, extend to the next atoll of rings. We find that bonds which are more than three bonds away—i.e., the smallest path from $\langle ij \rangle$ to $\langle kl \rangle$ consists of more than three bonds—have contributions, which are less then 0.5% of the main interaction. The distribution of the most important interactions for the case of stretch−stretch constants ($k^{rr}_{\langle 1,2 \rangle \langle kl \rangle}$) is shown in Figure 7.

This relatively localized picture of the force field is broadly compatible with the known chemistry of C_{60}. [60]-Fullerene replaces electron-deficient alkenes in organometallic complexes, undergoes halogenation and epoxidation, and dimerizes by [2 + 2]-addition, but does not react by η^5or η^6 addition to pentagonal or hexagonal faces. In many respects, the chemistry of C_{60} is closer to that of ethene than to that of a delocalized "super arene".[45]

Elaboration of the redundancy conditions does not yield exact zeros, though most values lie below 1.0 N/m. This is a consequence of the large uncertainties in several constants, and so, the conditions are essentially satisfied.

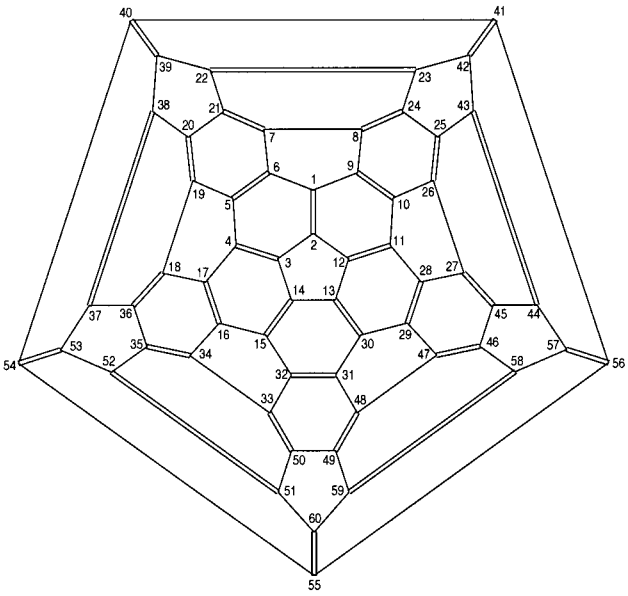

Figure 6. Atom labeling in C_{60}.[44]

In an earlier work on the force field in C_{60} by Quong et al.,[46] the Cartesian Hessian, obtained from a local density approximation, was used to calculate the force constant tensors between all pairs of atoms. The force constants were found to fall off with distance. However, a detailed comparison with the present model cannot be made since the force field by Quong et al. is decomposed into atom-to-atom interactions along the interatomic vectors. As compared to the present bond-to-bond interaction scheme, such an atom-to-atom approach is insensitive to the directional character of the polyhedral bonds.

5.3.3. Decomposition of the Wu Force Field into Slide and Stretch Terms. As compared to the complete force field, the methods which are traditionally used in chemistry are often seriously under-parametrized. The fitting procedure will then effectively "store" a number of different interactions in a few parameters. This implies that the force constants of such methods are "effective" force constants and must be interpreted with extreme caution. A good example is offered by the extended Wu force field. Its terms (eq 60) can be decomposed in slide and stretch terms. Decomposition of the potential in eq 60 using the values from Table 9 gives rise to the nonzero constants, listed in Table 11.

These constants satisfy the first two redundancy conditions (eqs 27 and 28) exactly and the next two (eqs 31 and 32) approximately. Note that although the stretching force constants c_1 and c_2 obtained by fitting the Wu force field are quite low, 520.1 and 348.1 N/m, the actual pure stretching interactions, as measured by the complete force field, are much higher, 762.2 and 650.2 N/m, and much more in accordance with the DFT results, 867.1 and 671.0 N/m, and with chemical experience.

Some constant values turn out to be degenerate, which reflects the fact that the Wu force field has fewer degrees of freedom than the complete one.

A clear shortcoming of the extended Wu force field is that it does not incorporate interactions between bonds which are three bonds away from each other, in contrast to the results of the complete force field. While the error on the frequencies is small, except for the lowest H_g mode, the too strongly localized character of the Wu force field will give less accurate eigenvectors for the vibrational modes.

TABLE 10: Constants for C_{60}, in Nm

stretch−stretch					stretch-slide					Slide-slide				
k	⟨*ij*⟩	⟨*kl*⟩	value	σ (%)	*k*	⟨*ij*⟩	⟨*kl*⟩	value	σ (%)	*k*	⟨*ij*⟩	⟨*kl*⟩	value	σ (%)
1	⟨1,2⟩	⟨1,2⟩	867.1	0.5	51	⟨1,2⟩	⟨1,6⟩	−140.7	2.3	114	⟨1,2⟩	⟨1,2⟩	574.9	1.3
2		⟨1,6⟩	59.8	3.4	52		⟨3,4⟩	83.1	2.3	115		⟨1,6⟩	288.4	1.6
3		⟨3,4⟩	−80.0	2.4	53		⟨3,14⟩	54.1	3.1	116		⟨3,4⟩	101.7	2.0
4		⟨3,14⟩	−51.3	3.3	54		⟨4,17⟩	8.6	2.2	117		⟨3,14⟩	58.0	2.9
5		⟨4,5⟩	24.1	1.6	55		⟨7,21⟩	−6.2	3.4	118		⟨4,5⟩	−10.3	5.7
6		⟨4,17⟩	1.9	8.9	56		⟨15,16⟩	−1.8	4.9	119		⟨4,17⟩	6.8	2.4
7		⟨7,8⟩	14.4	2.2	57		⟨15,32⟩	−3.8	2.4	120		⟨7,21⟩	3.9	8.6
8		⟨7,21⟩	16.6	1.1	58		⟨16,17⟩	5.9	1.6	121		⟨15,16⟩	−3.7	3.6
9		⟨15,16⟩	−0.1	58.0	59		⟨16,34⟩	−2.7	2.8	122		⟨15,32⟩	−1.7	7.0
10		⟨15,32⟩	4.9	1.4	60		⟨17,18⟩	−5.9	1.3	123		⟨16,17⟩	10.0	1.9
11		⟨16,17⟩	10.4	0.9	61		⟨18,36⟩	−0.5	25.7	124		⟨16,34⟩	−0.1	78.8
12		⟨16,34⟩	−0.4	18.1	62		⟨22,39⟩	0.4	23.3	125		⟨17,18⟩	−5.8	2.2
13		⟨17,18⟩	5.9	1.7	63		⟨33,34⟩	−1.8	4.0	126		⟨22,39⟩	0.1	78.5
14		⟨18,36⟩	−1.5	5.3	64		⟨33,50⟩	−0.8	11.6	127		⟨33,34⟩	−1.8	4.6
15		⟨22,39⟩	0.9	8.2	65		⟨34,35⟩	1.4	6.1	128		⟨33,50⟩	−2.0	4.1
16		⟨33,34⟩	−1.0	8.8	66		⟨35,36⟩	−1.1	6.9	129		⟨34,35⟩	0.2	50.8
17		⟨33,50⟩	1.0	8.5	67		⟨35,52⟩	−0.3	33.5	130		⟨35,36⟩	0.9	8.7
18		⟨34,35⟩	−1.2	8.2	68		⟨40,54⟩	0.1	58.8	131		⟨35,52⟩	1.0	8.9
19		⟨35,36⟩	0.3	36.8	69		⟨51,52⟩	0.1	64.8	132		⟨40,54⟩	−0.2	54.6
20		⟨35,52⟩	−1.2	6.6	70		⟨51,60⟩	−0.1	62.5	133		⟨51,52⟩	0.7	13.6
21		⟨40,41⟩	−0.5	21.3	71	⟨1,6⟩	⟨1,2⟩	−128.3	2.7	134		⟨51,60⟩	0.7	10.8
22		⟨40,54⟩	−0.9	11.8	72		⟨1,9⟩	−113.0	2.8	135		⟨52,53⟩	−0.9	9.3
23		⟨51,52⟩	0.4	23.2	73		⟨2,3⟩	66.1	2.9	136		⟨55,60⟩	1.8	6.9
24		⟨51,60⟩	0.2	47.1	74		⟨2,12⟩	40.7	3.7	137	⟨1,6⟩	⟨1,6⟩	500.6	1.1
25		⟨52,53⟩	1.0	7.8	75		⟨3,14⟩	5.1	3.8	138		⟨1,9⟩	263.0	1.6
26		⟨55,60⟩	−0.5	18.5	76		⟨7,8⟩	86.4	3.2	139		⟨2,3⟩	−78.9	2.9
27	⟨1,6⟩	⟨1,6⟩	671.0	0.4	77		⟨7,21⟩	52.4	3.2	140		⟨2,12⟩	−31.5	5.2
28		⟨1,9⟩	48.6	4.7	78		⟨8,24⟩	−2.2	15.4	141		⟨3,14⟩	−4.9	4.1
29		⟨2,3⟩	−69.8	2.2	79		⟨10,11⟩	−4.3	3.9	142		⟨7,8⟩	84.2	2.4
30		⟨2,12⟩	−25.2	5.6	80		⟨10,26⟩	−3.9	1.9	143		⟨10,26⟩	0.2	52.2
31		⟨3,14⟩	4.8	5.3	81		⟨11,12⟩	11.8	1.7	144		⟨11,28⟩	−3.5	2.4
32		⟨7,8⟩	−37.1	5.9	82		⟨11,28⟩	4.0	2.4	145		⟨13,14⟩	−3.6	3.1
33		⟨10,26⟩	13.8	0.7	83		⟨12,13⟩	−8.7	1.0	146		⟨15,16⟩	−1.8	6.7
34		⟨11,28⟩	−7.1	1.3	84		⟨13,14⟩	0.7	11.1	147		⟨15,32⟩	−0.7	12.2
35		⟨13,14⟩	5.7	2.3	85		⟨13,30⟩	−3.6	3.9	148		⟨22,39⟩	−5.6	1.6
36		⟨15,16⟩	3.5	3.5	86		⟨14,15⟩	−2.9	4.4	149		⟨23,42⟩	−1.6	4.2
37		⟨15,32⟩	−0.1	70.6	87		⟨15,32⟩	0.4	16.6	150		⟨29,47⟩	1.2	5.2
38		⟨22,39⟩	5.8	1.8	88		⟨22,23⟩	−3.1	2.8	151		⟨30,31⟩	2.1	2.5
39		⟨23,42⟩	−0.5	16.4	89		⟨22,39⟩	−4.1	1.9	152		⟨31,48⟩	−0.5	12.3
40		⟨29,47⟩	2.8	2.7	90		⟨23,24⟩	3.9	2.3	153		⟨32,33⟩	−0.2	25.9
41		⟨30,31⟩	−1.3	8.1	91		⟨23,42⟩	−1.6	6.2	154		⟨41,56⟩	0.3	26.0
42		⟨31,48⟩	−0.1	70.7	92		⟨27,28⟩	−1.6	4.7	155		⟨42,43⟩	3.2	2.0
43		⟨32,33⟩	−0.6	20.0	93		⟨27,45⟩	−1.9	5.8	156		⟨46,58⟩	0.6	9.8
44		⟨41,56⟩	0.4	22.1	94		⟨28,29⟩	2.4	4.3	157		⟨49,50⟩	−0.1	56.7
45		⟨42,43⟩	−1.3	11.9	95		⟨29,30⟩	−0.5	16.8	158		⟨49,59⟩	−0.4	22.1
46		⟨46,58⟩	1.0	12.1	96		⟨29,47⟩	0.4	22.4	159		⟨55,56⟩	0.6	14.4
47		⟨49,50⟩	0.2	44.0	97		⟨30,31⟩	−1.3	5.5	160		⟨59,60⟩	0.5	18.4
48		⟨49,59⟩	0.6	14.7	98		⟨31,32⟩	0.4	18.5					
49		⟨55,56⟩	−1.3	7.2	99		⟨31,48⟩	0.2	32.5					
50		⟨59,60⟩	−0.3	40.9	100		⟨32,33⟩	−0.8	8.7					
					101		⟨33,50⟩	1.4	8.9					
					102		⟨40,41⟩	0.5	13.8					
					103		⟨40,54⟩	0.5	15.0					
					104		⟨41,42⟩	−0.7	14.5					
					105		⟨41,56⟩	−0.1	71.1					
					106		⟨46,47⟩	0.5	20.4					
					107		⟨46,58⟩	0.1	83.6					
					108		⟨47,48⟩	−0.6	10.1					
					109		⟨48,49⟩	0.2	45.7					
					110		⟨49,50⟩	0.4	20.8					
					111		⟨49,59⟩	0.3	26.6					
					112		⟨55,56⟩	−0.1	60.7					
					113		⟨55,60⟩	−0.1	56.1					

6. Conclusion

A group-theoretical framework has been used to derive a complete force field for two extreme types of molecular cage: the deltahedron, for which all vibrations are bond stretches, and the trivalent polyhedral cage, for which bond stretches and bond slides describe all possible vibrational motions. Projection of ab initio calculated Hessian matrices allows comparison of the degree of localization in the force field in the two cases. Whereas the rigid B_{12} cage has significant cross cage interaction constants even for antipodal bonds, the force field of the trivalent C_{60} cage is dominated by slide and stretch constants for nearby bonds (separated by no more than three polyhedron edges). The latter result is compatible with the relatively localized π-addition chemistry of [60]-fullerene and suggests a parametrization of the force field for general fullerenes.

Acknowledgment. Research in Leuven was supported by the concerted action scheme of the Flemish Government (GOA, Ministerie van het Wetenschapsbeleid) and by the Flemish Science Foundation (FWO-Vlaanderen). P.W.F. is grateful for

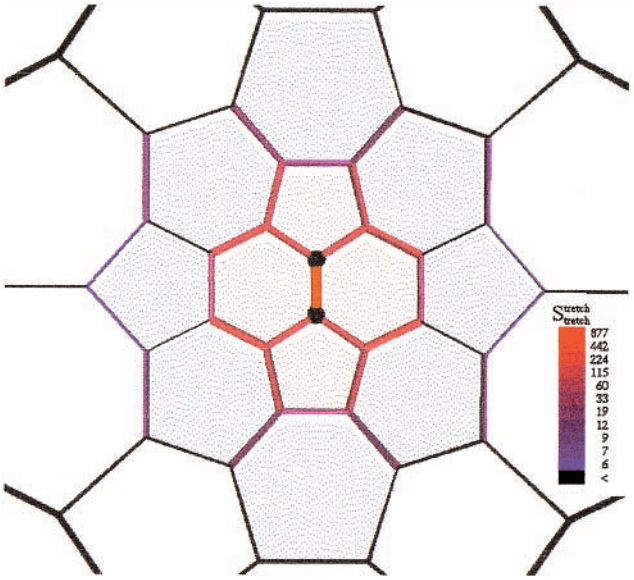

Figure 7. "Magnitude diagram" of the carbon skeleton in C_{60} for the $k^{rr}_{\langle 1,2\rangle\langle kl\rangle}$ force field constants. The red rings which encircle the central $\langle 1,2\rangle$ bond carry the most important interactions. The remaining interactions above 0.5% are found in the next circle of blue rings.

TABLE 11: Decomposition of Wu Force Field

stretch−stretch			stretch−slide			slide−slide		
$\langle ij\rangle$	$\langle kl\rangle$	value	$\langle ij\rangle$	$\langle kl\rangle$	value	$\langle ij\rangle$	$\langle kl\rangle$	value
⟨1,2⟩	⟨1,2⟩	762.2	⟨1,2⟩	⟨1,6⟩	−135.1	⟨1,2⟩	⟨1,2⟩	606.6
	⟨1,6⟩	41.6		⟨3,4⟩	88.0		⟨1,6⟩	337.9
	⟨3,4⟩	−50.4		⟨3,14⟩	52.1		⟨3,4⟩	125.5
	⟨3,14⟩	−38.7		⟨4,17⟩	−7.2		⟨3,14⟩	73.8
	⟨4,5⟩	49.4		⟨7,21⟩	−7.0		⟨4,5⟩	−49.4
	⟨4,17⟩	7.2	⟨1,6⟩	⟨1,2⟩	−142.1		⟨4,17⟩	−7.2
	⟨7,8⟩	21.0		⟨1,9⟩	−124.6		⟨7,21⟩	7.0
	⟨7,21⟩	7.0		⟨2,3⟩	98.4	⟨1,6⟩	⟨1,6⟩	601.3
⟨1,6⟩	⟨1,6⟩	650.2		⟨2,12⟩	50.6		⟨1,9⟩	321.4
	⟨1,9⟩	51.1		⟨3,14⟩	−10.9		⟨2,3⟩	−135.8
	⟨2,3⟩	−61.1		⟨7,8⟩	117.9		⟨2,12⟩	−64.6
	⟨2,12⟩	−36.7		⟨7,21⟩	60.4		⟨3,14⟩	10.9
	⟨3,14⟩	10.9		⟨8,9⟩	−21.0		⟨7,8⟩	108.9
	⟨7,8⟩	−8.6		⟨10,11⟩	−10.9		⟨10,26⟩	10.9
	⟨10,26⟩	10.9		⟨10,26⟩	−10.9			
				⟨11,12⟩	7.2			
				⟨12,13⟩	−10.9			

financial support under the EU TMR Networks USEFULL and BIOFULLERENES.

A Separation of Skeletal and Exohedral Vibrations in Binary Clusters of Type $(AX)_{v>}$

Consider a cluster with v atoms of type A, each of which has an additional bond to an atom X outside the cage. The q-coordinate basis of such a cluster consists of two subsets of displacements of atoms A and X, which will be arranged as shown in eq 63:

$$\mathbf{q} = \begin{pmatrix} \mathbf{q}^{A} \\ \mathbf{q}^{X} \end{pmatrix} \tag{63}$$

Accordingly, the total Hessian will be divided in four submatrices, depending on the type of atom which is being displaced:

$$\mathbf{H} = \begin{pmatrix} \mathbf{H}^{AA} & \mathbf{H}^{AX} \\ \mathbf{H}^{XA} & \mathbf{H}^{XX} \end{pmatrix} \tag{64}$$

The off-diagonal block matrices are related by transposition

$$\mathbf{H}^{AX} = (\mathbf{H}^{XA})^{\dagger} \tag{65}$$

The potential energy is thus given by

$$V = \frac{1}{2}\sum_{i,j} H_{ij}^{AA}\, q_i^{A}\, q_j^{A} + \sum_{i,j} H_{ij}^{AX}\, q_i^{A}\, q_j^{X} + \frac{1}{2}\sum_{i,j} H_{ij}^{XX}\, q_i^{X}\, q_j^{X} \tag{66}$$

where the indices i and j range from 1 to $3v$.

The kinetic energy is written as

$$T = \frac{1}{2} m_A \sum_i (\dot{q}_i^{A})^2 + \frac{1}{2} m_X \sum_i (\dot{q}_i^{X})^2 \tag{67}$$

where m_A and m_X are the respective masses of the atoms A and X.

The normal modes that result from the vibrational eigenvalue problem will be mixtures of skeletal vibrations and displacements of the exo atoms. For the purposes of constructing a force field for the cluster vibrations, we must project out the skeletal modes. This is done by requiring that the exohedral atoms follow the motions of the cluster atoms adiabatically, i.e., in such a way that the forces for the displacements of the exo atoms vanish.

For $\prime$ varying from 1 to $3v$, one has:

$$\frac{\partial V}{\partial q_{\prime}^{X}} = \sum_i H_{i\prime}^{AX}\, q_i^{A} + \sum_i H_{i\prime}^{XX}\, q_i^{X} = 0 \tag{68}$$

This condition can also be written as

$$\mathbf{H}^{XX}\mathbf{q}^{X} = -\mathbf{H}^{XA}\mathbf{q}^{A} \tag{69}$$

or

$$\mathbf{q}^{X} = -(\mathbf{H}^{XX})^{-1}\,\mathbf{H}^{XA}\mathbf{q}^{A} \tag{70}$$

$$\mathbf{q}^{X\dagger} = -\mathbf{q}^{A\dagger}\mathbf{H}^{AX}(\mathbf{H}^{XX})^{-1} \tag{71}$$

This expression shows how the exohedral atoms follow the displacement of the cluster atoms in a way which creates no extra force field. By substituting this result in the expression for the potential energy, we obtain an effective potential for the skeletal vibrations:

$$\begin{aligned} 2V_{\mathrm{eff}} &= \mathbf{q}^{A\dagger}\mathbf{H}^{AA}\mathbf{q}^{A} - 2\mathbf{q}^{A\dagger}\mathbf{H}^{AX}(\mathbf{H}^{XX})^{-1}\mathbf{H}^{XA}\mathbf{q}^{A} + \\ &\qquad \mathbf{q}^{A\dagger}\mathbf{H}^{AX}(\mathbf{H}^{XX})^{-1}\,\mathbf{H}^{XX}(\mathbf{H}^{XX})^{-1}\mathbf{H}^{XA}\mathbf{q}^{A} \\ &= \mathbf{q}^{A\dagger}[\mathbf{H}^{AA} - \mathbf{H}^{AX}(\mathbf{H}^{XX})^{-1}\mathbf{H}^{XA}]\mathbf{q}^{A} \end{aligned} \tag{72}$$

Here, the term in brackets is the effective Hessian, $\mathbf{H}_{\mathrm{eff}}$, from which the force field for the skeletal modes is to be extracted:

$$\mathbf{H}_{\mathrm{eff}} = \mathbf{H}^{AA} - \mathbf{H}^{AX}\,(\mathbf{H}^{XX})^{-1}\,\mathbf{H}^{XA} \tag{73}$$

For the calculation of the frequencies associated with these effective modes, we must introduce similar coordinate transformations for the time derivatives. The kinetic energy in matrix

$$\dot{\mathbf{q}}^{X} = -(\mathbf{H}^{XX})^{-1}\,\mathbf{H}^{XA}\dot{\mathbf{q}}^{A} \tag{74}$$

$$\dot{\mathbf{q}}^{X\dagger} = -\,\dot{\mathbf{q}}^{A\dagger}\,\mathbf{H}^{AX}\,(\mathbf{H}^{XX})^{-1} \tag{75}$$

form then becomes

$$2T = m_A\,\dot{\mathbf{q}}^{A\dagger}\,\dot{\mathbf{q}}^{A} + m_X\,\dot{\mathbf{q}}^{A\dagger}\,\mathbf{H}^{AX}(\mathbf{H}^{XX})^{-1}(\mathbf{H}^{XX})^{-1}\mathbf{H}^{XA}\dot{\mathbf{q}}^{A}$$
$$= \dot{\mathbf{q}}^{A\dagger}\,[m_A\mathbf{I} + m_X\mathbf{H}^{AX}(\mathbf{H}^{XX})^{-1}(\mathbf{H}^{XX})^{-1}\mathbf{H}^{XA}]\dot{\mathbf{q}}^{A} \quad (76)$$

The term in square brackets is the effective mass matrix, **M**:

$$\mathbf{M} = m_A\mathbf{I} + m_X\mathbf{H}^{AX}(\mathbf{H}^{XX})^{-1}(\mathbf{H}^{XX})^{-1}\mathbf{H}^{XA} \quad (77)$$

The frequencies ν of the effective modes are then obtained by solving the eigenvalue problem:

$$|\mathbf{H}_{eff} - 4\pi^2\nu^2\,\mathbf{M}| = 0 \quad (78)$$

The mass matrix **M** can be written as $\mathbf{S}_M^{-1}\mathbf{M}_d\mathbf{S}_M$, where $\mathbf{M}_d$ is the diagonalized mass matrix (all zeros, except for the eigenvalues on the diagonal) and $\mathbf{S}_M$ is the eigenvector matrix. Equation 72 thus becomes

$$2T = \dot{\mathbf{q}}^{A\dagger}\mathbf{S}_M^{-1}\mathbf{M}_d\mathbf{S}_M\dot{\mathbf{q}}^{A}$$
$$= \dot{\tilde{\mathbf{q}}}^{A\dagger}\mathbf{M}_d\dot{\tilde{\mathbf{q}}}^{A}$$
$$= \dot{\hat{\mathbf{q}}}^{A\dagger}\dot{\hat{\mathbf{q}}}^{A} \quad (79)$$

$\tilde{\mathbf{q}}^A = \mathbf{S}_M\mathbf{q}^A$ are mass-weighted coordinates, and $\hat{\mathbf{q}}^A = \sqrt{\mathbf{M}_d}\mathbf{S}_M\mathbf{q}^A$, or

$$\mathbf{q}^A = \mathbf{S}_M^{-1}\frac{1}{\sqrt{\mathbf{M}_d}}\hat{\mathbf{q}}^A \quad (80)$$

By substituting eq 80 in eq 72, we obtain

$$2V_{eff} = \hat{\mathbf{q}}^{A\dagger}\left[\frac{1}{\sqrt{\mathbf{M}_d}}\mathbf{S}_M(\mathbf{H}^{AA} - \mathbf{H}^{AX}\,(\mathbf{H}^{XX})^{-1}\,\mathbf{H}^{XA})\mathbf{S}_M^{-1}\frac{1}{\sqrt{\mathbf{M}_d}}\right]\hat{\mathbf{q}}^A \quad (81)$$

Diagonalization of the term in square brackets yields the solutions of the eigenvalue problem in eq 78.

For the purpose of conversion from Cartesian coordinates to internal and collective coordinates, new equilibrium positions for the "(AX)" atoms have to be calculated. The following transformation was used:

$$q_i^{AX}(m_A + m_X) = q_i^A m_A + q_i^X m_X \quad (82)$$

References and Notes

(1) Ceulemans, A.; Fowler, P. W. *Nature* **1991**, *353*, 52−54.
(2) Fowler, P. W.; Quinn, C. M. *Theor. Chim. Acta* **1986**, *70*, 333−350.
(3) Altmann, S. L. *Induced Representations in Crystals and Molecules*; Academic: London, 1977.
(4) Wilson, E. B., Jr.; Decius, J. C.; Cross, P. C. *Molecular Vibrations*; McGraw Hill: New York, 1955.
(5) Lipscomb, W. N. *Science* **1977**, *196*, 1047−1055.
(6) Boyle, L. L.; Parker, Y. M. *Mol. Phys.* **1980**, *39*, 95−109.
(7) Cauchy, A. L. *J. Ecole Impériale Polytech.* **1813**, *19*, 87−98.
(8) *Gmelin Handbuch der Anorganische Chemie*; Springer-Verlag: Berlin, 1979; Volume 54, Borverbindungen, Part 20.3.
(9) Brint, P.; Sangchakr, B.; Fowler, P. W. *J. Chem. Soc., Faraday Trans. 2* **1989**, *85*, 29−37.
(10) Brint, P.; Sangchakr, B.; Fowler, P. W.; Weldon, V. J. *J. Chem. Soc. Dalton Trans.* **1989**, 2253−2260.
(11) Andzelm, J.; Wimmer, E. *J. Chem. Phys.* **1992**, *96*, 1280. *DGauss 4.0*; Oxford Molecular, Ltd.: Beaverton, OR, 1997.
(12) UniChem is a registered trademark of Oxford Molecular Group.
(13) Muetterties, E. L.; Merrifield, R. E.; Miller, H. C.; Knoth, W. H., Jr.; Downing, J. R. *J. Am. Chem. Soc.* **1962**, *84*, 2506−2508.
(14) Leites, L. A.; Bukalov, S. S.; Kurbakova, A. P.; Kaganski, M. M.; Gaft, Y. L.; Kuznetsov, N. T.; Zakharova, I. A. *Spectrochim. Acta* **1982**, *38A*, 1047−1056.
(15) Weber, W.; Thorpe, M. F. *J. Phys. Chem. Solids* **1975**, *36*, 967.
(16) Abdul-Fattah, M.; Butler, I. S. *Can. J. Spectrosc.* **1977**, *22*, 110.
(17) Eaton, P. E.; Cole, T. W., Jr. *J. Am. Chem. Soc.* **1964**, *86*, 962−964.
(18) Fleischer, E. B. *J. Am. Chem. Soc.* **1964**, *86*, 3889−3890.
(19) Della, E. W.; McCoy, E. F.; Patney, H. K.; Jones, G. L.; Miller, F. A. *J. Am. Chem. Soc.* **1979**, *101*, 7441−7457.
(20) Cole, T. W., Jr.; Perkins, J.; Putnam, S.; Pakes, P. W.; Strauss, H. L. *J. Phys. Chem.* **1981**, *85*, 2185−2189.
(21) Kovačević, K.; Maksić, Z. B. *J. Org. Chem.* **1974**, *39*, 539−557.
(22) Bischof, P.; Eaton, P. E.; Gleiter, R.; Heilbronner, E.; Jones, T. B.; Musso, H.; Schmelzer, A.; Stober, R. *Helv. Chim. Acta* **1978**, *61*, 547−557.
(23) Schubert, W.; Yoshimine, M.; Pacansky, J. *J. Phys. Chem.* **1981**, *85*, 1340−1342.
(24) Almlöf, J.; Jonvik, T. *Chem. Phys. Lett.* **1982**, *92*, 267−270.
(25) Frisch, M. J.; Trucks, G. W.; Schlegel, H. B.; Gill, P. M. W.; Johnson, B. G.; Robb, M. A.; Cheeseman, J. R.; Keith, T.; Petersson, G. A.; Montgomery, J. A.; Raghavachari, K.; Al-Laham, M. A.; Zakrzewski, V. G.; Ortiz, J. V.; Foresman, J. B.; Cioslowski, J.; Stefanov, B. B.; Nanayakkara, A.; Challacombe, M.; Peng, C. Y.; Ayala, P. Y.; Chen, W.; Wong, M. W.; Andres, J. L.; Replogle, E. S.; Gomperts, R.; Martin, R. L.; Fox, D. J.; Binkley, J. S.; Defrees, D. J.; Baker, J.; Stewart, J. P.; Head-Gordon, M.; Gonzalez, C.; Pople, J. A. *Gaussian 94, Revision C.3*; Gaussian, Inc.: Pittsburgh, PA, 1995.
(26) Dunning, T. H., Jr.; Hay, P. J. In *Modern Theoretical Chemistry*; Schaefer, H. F., III, Ed.; Plenum: New York, 1976; pp 1−28.
(27) Becke, A. D. *J. Chem. Phys.* **1993**, *98*, 5648−5652.
(28) Kroto, H. W.; Heath, J. R.; O'Brien, S. C.; Curl, R. F.; Smalley, R. E. *Nature* **1985**, *318*, 162−163.
(29) Bethune, D. S.; Meijer, G.; Tang, W. C.; Rosen. H. J. *Chem. Phys. Lett.* **1990**, *174*, 219−222.
(30) Coulombeau, C.; Jobic, H.; Bernier, P.; Fabre, C.; Schutz, D.; Rassat, A. *J. Phys. Chem.* **1992**, *96*, 22−24.
(31) Chase, B.; Fagan, P. J. *J. Am. Chem. Soc.* **1992**, *114*, 2252−2256.
(32) Chase, B.; Herron, N.; Holler, E. *J. Phys. Chem.* **1992**, *96*, 4262−4266.
(33) Wang, K.-A.; Rao, A. M.; Eklund, P. C.; Dresselhaus, M. S.; Dresselhaus, G. *Phys. Rev. B* **1993**, *48*, 11375.
(34) Dong, Z.-H.; Zhou, P.; Holden, J. M.; Eklund, P. C.; Dresselhaus, M. S.; Dresselhaus, G. *Phys. Rev. B* **1993**, *48*, 2862.
(35) van den Heuvel, D. J.; van den Berg, G. J. B.; Groenen, E. J. J.; Schmidt, J.; Holleman, I.; Meijer, G. *J. Phys. Chem.* **1995**, *99*, 11644−11649.
(36) Negri, F.; Orlandi, G.; Zerbetto, F. *Chem. Phys. Lett.* **1992**, *190*, 174−178.
(37) Dixon, D. A.; Chase, B. E.; Fitzgerald, G.; Matsuzawa, N. *J. Phys. Chem.* **1995**, *99*, 4486−4489. The authors wish to thank G. F. for providing the full Hessian from this calculation.
(38) Liu, S.; Lu, Y.-J.; Kappes, M. M.; Ibers, J. A. *Science* **1991**, *254*, 408−410.
(39) Wu, Z. C.; Jelski, D. A.; George, T. F. *Chem. Phys. Lett.* **1987**, *137*, 291−294.
(40) Jishi, R. A.; Mirie, R. M.; Dresselhaus, M. S. *Phys. Rev. B* **1992**, *45*, 13685.
(41) Ceulemans, A.; Fowler, P. W.; Vos, I. *J. Chem. Phys.* **1994**, *100*, 5491−5500.
(42) Dresselhaus, M. S.; Dresselhaus, G.; Eklund, P. C. *Science of Fullerenes and Carbon Nanotubes*; Academic Press: San Diego, 1996.
(43) Green, W. H., Jr.; Gorun, S. M.; Fitzgerald, G.; Fowler, P. W.; Ceulemans, A.; Titeca, B. C. *J. Phys. Chem.* **1996**, *100*, 14892−14898.
(44) Godley, E. W.; Taylor, R. *Pure Appl. Chem.* **1997**, *69*, 1411−1434.
(45) Taylor, R. *Lecture Notes on Fullerene Chemistry: A Handbook for Chemists*; Imperial College Press: London, 1999.
(46) Quong, A. A.; Pederson, M. R.; Feldman, J. L. *Solid State Commun.* **1993**, *87*, 535−539.